Exceptionally High Stability of Copolymer-Templated Ordered Silica with Large Cage-Like Mesopores

Michal Kruk, Ewa B. Celer, and Mietek Jaroniec*

Department of Chemistry, Kent State University, Kent, Ohio 44242

Received September 24, 2003. Revised Manuscript Received December 10, 2003

FDU-1 silicas with large (∼10 nm) cage-like mesopores were synthesized under acidic conditions using a poly(ethylene oxide)−poly(butylene oxide)−poly(ethylene oxide) triblock copolymer template. Structural changes caused by heating in water at 373 K for different periods of time (from 3 hours to 32 days) and by calcination at 973−1273 K were investigated in order to assess the hydrothermal and thermal stability of FDU-1. It was shown that FDU-1 exhibits a hydrothermal stability unprecedented among ordered mesoporous silicas (OMSs), because it retains its uniform mesopores even after 32 days of heating in water at 373 K, which is by one or two orders of magnitude longer than in the case of typical OMSs and at least two times longer than in the reported cases of the most stable OMSs. This exceptional hydrothermal stability of FDU-1 can be attributed to the combination of its extremely large average wall thickness and the continuous 3-dimensional nature of its thick wall backbone. The boiling water appears to gradually peel off the surface layers of silica, but even the removal of a 1-nm-thick layer does not compromise the integrity of the FDU-1 framework. The dissolution of silica appears to take place much faster in the region of the pore entrances, because the latter undergo a significant enlargement as the hydrothermal treatment is prolonged, and, consequently, samples treated for very long times exhibit relatively open pore structures. The FDU-1 structure can be made even more hydrothermally stable when an additional layer of silica is introduced on its surface or its framework is made more consolidated by increasing the calcination temperature to 1173 K. Moreover, the introduction of hydrophobic surface groups can enhance the hydrothermal stability so much that the pore structure is almost unchanged after boiling in water for 4 days. It appears that the presence of a compact layer of hydrophobic groups on the silica surface successfully prevents its erosion in boiling water. FDU-1 exhibits a facile thermal stability. More than 70% of the primary mesopore volume was retained after calcination at 1173 K of the FDU-1 sample obtained in a relatively short (30-hour), two-step synthesis.

Introduction

Over the past decade, we have witnessed an explosive growth of research on the synthesis of ordered mesoporous materials (OMMs),[1−20] initiated by the pioneering works of Kresge and co-workers,[21,22] and Kuroda, Inagaki, and co-workers[23,24] on the synthesis of ordered mesoporous silicas (OMSs). Because of their high specific surface areas, large mesopore volumes, tailorable pore diameters, and structure symmetry, OMMs of various framework compositions are very attractive from the point of view of many applications in fields such as catalysis, separations, adsorption, immobilization of biomolecules, and manufacturing of electronic, sensing, and optical devices.[1−20] In many of these applications, high hydrothermal and/or thermal stability is required. Although OMSs, which currently constitute the most prominent group of OMMs, often exhibit a relatively good thermal stability,[24−26] their hydrother-

* To whom correspondence should be addressed. Phone: (330) 672-3790. Fax: (330) 672-3816. E-mail: jaroniec@kent.edu.

(1) Raman, N. K.; Anderson, M. T.; Brinker, C. J. *Chem. Mater.* **1996**, *8*, 1682.
(2) Sayari, A. *Stud. Surf. Sci. Catal.* **1996**, *102*, 1.
(3) Sayari, A. *Chem. Mater.* **1996**, *8*, 1840.
(4) Corma, A. *Chem. Rev.* **1997**, *97*, 2373.
(5) Moller, K.; Bein, T. *Chem. Mater.* **1998**, *10*, 2950.
(6) Ying, J. Y.; Mehnert, C. P.; Wong, M. S. *Angew. Chem., Int. Ed.* **1999**, *38*, 56.
(7) Stein, A.; Melde, B. J.; Schroden, R. C. *Adv. Mater.* **2000**, *12*, 1403.
(8) Sayari, A.; Hamoudi, S. *Chem. Mater.* **2001**, *13*, 3151.
(9) Schuth, F. *Chem. Mater.* **2001**, *13*, 3184.
(10) Trong On, D.; Desplantier-Giscard, D.; Kaliaguine, S. *Appl. Catal., A* **2001**, *222*, 299.
(11) Ryoo, R.; Joo, S. H.; Kruk, M.; Jaroniec, M. *Adv. Mater.* **2001**, *13*, 677.
(12) Davis, M. E. *Nature* **2002**, *417*, 813.
(13) Soler-Illia, G. J. de A. A.; Sanchez, C.; Lebeau, B.; Patarin, J. *Chem. Rev.* **2002**, *102*, 4093.
(14) Polarz, S.; Antonietti, M. *Chem. Commun.* **2002**, 2593.
(15) Wright, A. P.; Davis, M. E. *Chem. Rev.* **2002**, *102*, 3589.
(16) De Vos, D. E.; Dams, M.; Sels, B. F.; Jacobs, P. A. *Chem. Rev.* **2002**, *102*, 3615.
(17) Schuth, F.; Schmidt, W. *Adv. Mater.* **2002**, *14*, 629.
(18) He, X.; Antonelli, D. *Angew. Chem., Int. Ed.* **2002**, *41*, 214.
(19) Liu, Y.; Pinnavaia, T. J. *J. Mater. Chem.* **2002**, *12*, 3179.
(20) Stein, A. *Adv. Mater.* **2003**, *15*, 763.
(21) Kresge, C. T.; Leonowicz, M. E.; Roth, W. J.; Vartuli, J. C.; Beck, J. S. *Nature* **1992**, *359*, 710.
(22) Beck, J. S.; Vartuli, J. C.; Roth, W. J.; Leonowicz, M. E.; Kresge, C. T.; Schmitt, K. D.; Chu, C. T.-W.; Olson, D. H.; Sheppard, E. W.; McCullen, S. B.; Higgins, J. B.; Schlenker, J. L. *J. Am. Chem. Soc.* **1992**, *114*, 10834.
(23) Yanagisawa, T.; Shimizu, T.; Kuroda, K.; Kato, C. *Bull. Chem. Soc. Jpn.* **1990**, *63*, 988.
(24) Inagaki, S.; Fukushima, Y.; Kuroda, K. *J. Chem. Soc., Chem. Commun.* **1993**, 680.

10.1021/cm034911u CCC: $27.50
Published on Web 01/24/2004

mal stability (in particular, at high temperature in the presence of water vapor or in hot aqueous media) is often unsatisfactory.[27−32] Poor hydrothermal stability, in addition to low acidity, hinders the application of OMSs in the petrochemical processing of heavy feedstocks, where OMSs are highly promising because of their relatively large pore size.[19] Therefore, the assessment of the hydrothermal and thermal stability of OMSs aimed at the identification of the stable materials, and the elucidation of the factors that govern the stability, as well as the synthesis of more stable OMSs have become major areas of research on OMMs.[19,24−40]

Although factors that determine the hydrothermal stability of OMSs are still to be fully elucidated,[41,42] several prominent ones have been identified. It is clear that the hydrothermal stability in boiling water tends to be higher for materials with larger pore wall thickness[34] and with more condensed frameworks.[35,43] Because of the fact that the collapse of OMSs in the presence of water involves the hydrolysis of siloxane bridges (Si−O−Si),[33] the higher extent of the framework condensation implies that a larger number of siloxanes have to be hydrolyzed to compromise the framework integrity. The effect of the larger pore wall thickness is likely to be quite analogous, because in the case of thicker walls, the thicker layer of silica has to be ruptured or dissolved (both of which involve the hydrolysis of siloxane bridges) to cause the structural disintegration. The introduction of heteroatoms, such as aluminum, on the surface or in the framework of OMSs often resulted in enhanced hydrothermal stability.[36,37,39,42,44−47] The presence of zeolite-like secondary structural subunits in the OMS framework or the coating of the OMS surface with zeolite species also improved the hydrothermal stability.[19,28−30,38,40,48−53] Another way to improve the stability is to introduce a hydrophobic coating, for instance a monolayer of organosilane ligands, on the OMS surface.[33,54−56] The stabilization in the above cases can be explained as an effect of either the introduction of the protective layer on the OMS surface,[33,38,40,47,54−56] which prevents the erosion of the silica framework, or the improvement of the inherent stability of the silicate framework through the introduction of more stable structural units[28−30] or the doping of heteroatoms.[42] Typically, OMSs lose their ordered porous structures during heating in water at 373 K for several hours,[31,57] although in some cases the ordered porosity was retained for much longer.[30,34−38,42−46,48−52,58−68] The most stable currently known OMSs contain heteroatoms (primarily aluminum) on their surface[36,38−40,44,45] or in their framework,[30,37,48,49,52,53] for instance in the form of zeolite-like secondary structural subunits,[30,44,48,49,52,53] or exhibit extremely thick pore walls.[35,67] In particular, a 2-dimensional hexagonally ordered aluminosilicate with zeolite-like structural subunits retained its periodic structure after 12.5 days of boiling in water, as seen from X-ray diffraction (XRD).[30] FDU-1 silica with very thick pore walls (as will be discussed hereafter) was reported to exhibit several peaks in its XRD pattern after 9 days of boiling.[67] Unfortunately, XRD is not the best method to study the structural stability of OMSs[42,56,69] because it was shown to indicate a significant retention of the periodic structure even for samples whose porous structures underwent a dramatic structural degradation. Nonetheless, the above XRD data suggest very high hydrothermal stability for the materials mentioned above. Gas adsorption, which is considered to be more reliable than XRD for the assessment of the structural stability,[42,56,69] showed that some aluminosilicates retained accessible uniform mesoporosity after a week of boiling in water and some residual accessible mesopores after a month of boiling.[45]

(25) Chen, C.-Y.; Li, H.-X.; Davis, M. E. *Microporous Mater.* **1993**, *2*, 17.
(26) Chen, C.-Y.; Xiao, S.-Q.; Davis, M. E. *Microporous Mater.* **1995**, *4*, 1.
(27) McCullen, S. B.; Vartuli, J. C. Mobil Oil Co. U.S. Patent 5,156,829, 1992.
(28) Liu, Y.; Zhang, W.; Pinnavaia, T. J. *J. Am. Chem. Soc.* **2000**, *122*, 8791.
(29) Liu, Y.; Zhang, W.; Pinnavaia, T. J. *Angew. Chem., Int. Ed.* **2001**, *40*, 1255.
(30) Zhang, Z.; Han, Y.; Zhu, L.; Wang, R.; Yu, Y.; Qiu, S.; Zhao, D.; Xiao, F.-S. *Angew. Chem., Int. Ed.* **2001**, *40*, 1258.
(31) Ryoo, R.; Kim, J. M.; Ko, C. H.; Shin, C. H. *J. Phys. Chem. B* **1996**, *100*, 17718.
(32) Ryoo, R.; Jun, S. *J. Phys. Chem. B* **1997**, *101*, 317.
(33) Koyano, K. A.; Tatsumi, T.; Tanaka, Y.; Nakata, S. *J. Phys. Chem. B* **1997**, *101*, 9436.
(34) Zhao, D.; Feng, J.; Huo, Q.; Melosh, N.; Fredrickson, G. H.; Chmelka, B. F.; Stucky, G. D. *Science* **1998**, *279*, 548.
(35) Kim, S. S.; Zhang, W.; Pinnavaia, T. J. *Science* **1998**, *282*, 1302.
(36) Mokaya, R. *Angew. Chem., Int. Ed.* **1999**, *38*, 2930.
(37) Shen, S.-C.; Kawi, S. *J. Phys. Chem. B* **1999**, *103*, 8870.
(38) Trong On, D.; Kaliaguine, S. *Angew. Chem., Int. Ed.* **2002**, *41*, 1036.
(39) O'Neil, A. S.; Mokaya, R.; Poliakoff, M. *J. Am. Chem. Soc.* **2002**, *124*, 10636.
(40) Trong On, D.; Kaliaguine, S. *J. Am. Chem. Soc.* **2003**, *125*, 618.
(41) Kim, J. M.; Jun, S.; Ryoo, R. *J. Phys. Chem. B* **1999**, *103*, 6200.
(42) Han, Y.; Li, N.; Zhao, L.; Li, D.; Xu, X.; Wu, S.; Di, Y.; Li, C.; Zou, Y.; Yu, Y.; Xiao, F.-S. *J. Phys. Chem. B* **2003**, *107*, 7551.
(43) Mokaya, R. *J. Phys. Chem. B* **1999**, *103*, 10204.
(44) Kawi, S.; Shen, S. C. *Stud. Surf. Sci. Catal.* **2000**, *129*, 227.
(45) Shen, S.-C.; Kawi, S. *Langmuir* **2002**, *18*, 4720.
(46) Mal, N. K.; Kumar, P.; Fujiwara, M.; Kuraoka, K. *Stud. Surf. Sci. Catal.* **2002**, *142*, 1307.
(47) Mokaya, R. *ChemPhysChem* **2002**, *3*, 360.
(48) Li, Y.; Shi, J.; Hua, Z.; Chen, H.; Ruan, M.; Yan, D. *Nano Lett.* **2003**, *3*, 609.
(49) Han, Y.; Wu, S.; Sun, Y.; Li, D.; Xiao, F.-S.; Liu, J.; Zhang, X. *Chem. Mater.* **2002**, *14*, 1144.
(50) Xiao, F.-S.; Han, Y.; Yu, Y.; Meng, X.; Yang, M.; Wu, S. *J. Am. Chem. Soc.* **2002**, *124*, 888.
(51) Liu, J.; Zhang, X.; Han, Y.; Xiao, F.-S. *Chem. Mater.* **2002**, *14*, 2536.
(52) Zheng, J.; Zhang, Y.; Li, Z.; Wei, W.; Wu, D.; Sun, Y. *Chem. Phys. Lett.* **2003**, *376*, 136.
(53) Liu, Y.; Pinnavaia, T. J. *Chem. Mater.* **2002**, *14*, 3.
(54) Lim, M. H.; Stein, A. *Chem. Mater.* **1999**, *11*, 3285.
(55) Zhao, X. S.; Lu, G. Q.; Hu, X. *Microporous Mesoporous Mater.* **2000**, *41*, 37.
(56) Kisler, J. M.; Gee, M. L.; Stevens, G. W.; O'Connor, A. *J. Chem. Mater.* **2003**, *15*, 619.
(57) Zhao, D.; Huo, Q.; Feng, J.; Chmelka, B. F.; Stucky, G. D. *J. Am. Chem. Soc.* **1998**, *120*, 6024.
(58) Das, D.; Tsai, C.-M.; Cheng, S. *Chem. Commun.* **1999**, 473.
(59) Das, D.; Tsai, C.-M.; Cheng, S. *Stud. Surf. Sci. Catal.* **2000**, *129*, 85.
(60) Xia, Q.-H.; Hidajat, K.; Kawi, S. *Mater. Lett.* **2000**, *42*, 102.
(61) Mori, T.; Kuroda, Y.; Yoshikawa, Y.; Nagao, M.; Kittaka, S. *Langmuir* **2002**, *18*, 1595.
(62) Mal, N. K.; Kumar, P.; Fujiwara, M. *Stud. Surf. Sci. Catal.* **2002**, *141*, 445.
(63) Yu, J.; Shi, J.-L.; Chen, H.-R.; Yan, J.-N.; Yan, D.-S. *Microporous Mesoporous Mater.* **2001**, *46*, 153.
(64) Xia, Q.-H.; Hidajat, K.; Kawi, S. *Chem. Lett.* **2001**, 654.
(65) Chan, Y.-T.; Lin, H.-P.; Mou, C.-Y.; Liu, S.-T. *Chem. Commun.* **2002**, 2878.
(66) Kim, S.-S.; Liu, Y.; Pinnavaia, T. J. *Microporous Mesoporous Mater.* **2001**, *44*−*45*, 489.
(67) Yu, C.; Yu, Y.; Zhao, D. *Chem. Commun.* **2000**, 575.
(68) Schmidt-Winkel, P.; Lukens, W. W., Jr.; Yang, P.; Margolese, D. I.; Lettow, J. S.; Ying, J. Y.; Stucky, G. D. *Chem. Mater.* **2000**, *12*, 686.
(69) Kruk, M.; Jaroniec, M.; Sayari, A. *Microporous Mesoporous Mater.* **1999**, *27*, 217.

The factors governing the thermal stability of OMSs are also not fully elucidated. Some OMSs were found to be inherently very thermally stable under anhydrous atmosphere,[24,26,35,66,70−72] which in certain cases appeared to be clearly related to their high degree of framework cross-linking.[26,35] These OMSs were found to be stable at 1273 K for several hours under anhydrous atmosphere. Their stability above 1273 K was sometimes reported,[26,73] but it is not clear whether the thermal treatments were comparably long in these cases. The structural collapse of OMSs at very high temperatures is not only temperature-dependent, but also time-dependent (see data reported in ref 70) and thus the actual stability of these apparently more stable OMSs[26,73] may be similar to that of the aforementioned OMSs stable at 1273 K for several hours. Many reports focused on the hydrothermal stability under steam atmosphere.[28−31,38−40,47,53,74] In these cases, the benchmark stability was a retention of the structure after steaming at 1173 K for several hours, which, on the basis of the literature data,[71] is likely to be equivalent to heating to at least 1273 under an atmosphere of dry nitrogen or air. High thermal stability of OMSs can be imparted by the increase in the pore wall thickness,[72,74] the recrystallization,[43] or the proper introduction of aluminum heteroatoms.[39,47]

Although much work has been devoted to the assessment and improvement of the thermal and hydrothermal stability of OMSs, most studies were focused on materials with channel-like pores, either straight or branched. Very little work[67,75−77] was focused on an important group of OMSs with cage-like pores.[78−80] These OMSs have attracted a significant attention because of their remarkable three-dimensional (3-D) mesopore structures that are particularly suitable for applications requiring the use of thin films and fibers with accessible mesoporosity.[81,82] More recently, wide opportunities in the pore size and pore entrance size control using commercially available block copolymer templates were reported[83−85] and molecular sieving properties of some OMSs with cage-like pores were documented.[86] OMSs with cage-like pores and multidirectional pore systems are suitable as catalyst supports, molecular sieves, templates for advanced nanostructures,[11,85] and hosts for biomolecules[85] and nanoobjects, such as quantum dots.[87] We are aware of only two reports that provide some insight into the thermal stability of OMSs with cage-like pores at temperatures up to 1123 K,[75,76] and two reports on the hydrothermal stability of these materials,[67,77] including the aforementioned work on FDU-1.[67] There were several reports on the stability of silica mesocellular foams (MCFs) with uniform cage-like mesopores,[40,53,68] but MCFs are disordered or weakly ordered materials. It is clear that there is a need for better assessment and appreciation of thermal and hydrothermal stability of OMSs with cage-like pores.

The present contribution provides an account of an unprecedented hydrothermal stability of FDU-1, in which uniform mesoporosity is retained even after 32 days of heating in water at 373 K (longer times were not studied). The methods suitable to enhance the hydrothermal stability are demonstrated, including the surface modification and high-temperature calcination. The explanation of the unprecedented hydrothermal stability of FDU-1 was suggested. The thermal stability of FDU-1 was also elucidated.

Experimental Section

Materials. FDU-1 silicas were synthesized under acidic conditions using a poly(ethylene oxide)−poly(butylene oxide)−poly(ethylene oxide) triblock copolymer template ($EO_{39}BO_{47}$-EO_{39}, B50-6600, Dow Chemical), as reported in detail elsewhere.[67,84] FDU-1 exhibits a cubic *Fm*3*m* structure (face-centered cubic, cubic close-packed) (see the transmission electron microscopy image in Figure 1) with stacking faults related to the occurrence of hexagonal close-packed (3-D hexagonal) intergrowth.[84] In this close-packed structure, each spherical pore is expected to be connected to its twelve nearest-neighbor pores. Sample I was synthesized at room temperature. Samples IIa−e were synthesized initially at room temperature (as in the case of sample I) and subsequently the synthesis mixture was transferred to a Teflon-lined autoclave and heated at 373 K for 6 h. Sample III was synthesized in a similar way, but heated at 353 K for 8 days. The as-synthesized FDU-1 samples (that is, the copolymer−silica composites) were calcined under air for 5 h at 813 K (the heating rate was 1 K min^{-1}). Alternatively, the calcination temperature was set to a higher value in the range from 973 to 1273 K (the heating rate and the dwell time were the same as above). The samples calcined at temperatures higher than 813 K are denoted X-Cy, where X stands for the sample used (e.g., I, IIa−e or III) and y indicates the calcination temperature in Kelvin degrees. Surfaces of selected samples were modified through the chemical bonding of trimethylsilyl (TMS) ligands. The modification was carried out using trimethylchlorosilane in pyridine under reflux conditions, as described elsewhere.[88] The modified samples are denoted X-TMS. One of the TMS-modified samples (IId-TMS) was calcined under air at 813 K to eliminate the methyl groups from the TMS ligands. The resulting sample is denoted IId-TMS-C. Selected samples (usually about 100 mg) were dispersed in deionized water (40 mL) and heated in a Teflon-lined autoclave at 373 K for different periods of time ranging from 3 hours to 32 days. Herein, this procedure will be referred to as "boiling". After the boiling, the samples were

(70) Naono, H.; Hakuman, M.; Shiono, T. *J. Colloid Interface Sci.* **1997**, *186*, 360.
(71) Namba, S.; Mochizuki, A. *Res. Chem. Intermed.* **1998**, *24*, 561.
(72) Mokaya, R. *J. Mater. Chem.* **2002**, *12*, 3027.
(73) Li, W.; Yao, Y.; Wang, Z.; Zhao, J.; Zhao, M.; Sun, C. *Mater. Chem. Phys.* **2001**, *70*, 144.
(74) Mokaya, R. *Chem. Commun.* **2001**, 933.
(75) Goletto, V.; Imperor, M.; Babonneau, F. *Stud. Surf. Sci. Catal.* [CD-ROM] **2001**, *135*.
(76) Huang, L.; Wind, S. J.; O'Brian, S. P. *Nano Lett.* **2003**, *3*, 299.
(77) Newalkar, B. L.; Komarneni, S.; Turaga, U. T.; Katsuki, H. *J. Mater. Chem.* **2003**, *13*, 1710.
(78) Huo, Q.; Margolese, D. I.; Ciesla, U.; Feng, P.; Gier, T. E.; Sieger, P.; Leon, R.; Petroff, P. M.; Schuth, F.; Stucky, G. D. *Nature* **1994**, *368*, 317.
(79) Huo, Q.; Leon, R.; Petroff, P. M.; Stucky, G. D. *Science* **1995**, *268*, 1324.
(80) Sakamoto, Y.; Kaneda, M.; Terasaki, O.; Zhao, D. Y.; Kim, J. M.; Stucky, G. D.; Shin, H. J.; Ryoo, R. *Nature* **2000**, *408*, 449.
(81) Zhao, D.; Yang, P.; Melosh, N.; Feng, J.; Chmelka, B. F.; Stucky, G. D. *Adv. Mater.* **1998**, *10*, 1380.
(82) Yang, P.; Zhao, D.; Chmelka, B. F.; Stucky, G. D. *Chem. Mater.* **1998**, *10*, 2033.
(83) Kruk, M.; Antochshuk, V.; Matos, J. R.; Mercuri, L. P.; Jaroniec, M. *J. Am. Chem. Soc.* **2002**, *124*, 768.
(84) Matos, J. R.; Kruk, M.; Mercuri, L. P.; Jaroniec, M.; Zhao, L.; Kamiyama, T.; Terasaki, O.; Pinnavaia, T. J.; Liu, Y. *J. Am. Chem. Soc.* **2003**, *125*, 821.
(85) Fan, J.; Yu, C.; Gao, F.; Lei, J.; Tian, B.; Wang, L.; Luo, Q.; Tu, B.; Zhou, W.; Zhao, D. *Angew. Chem., Int. Ed.* **2003**, *42*, 3146.
(86) Hunter, H. M. A.; Garcia-Bennett, A. E.; Shannon, I. J.; Zhou, W.; Wright, P. A. *J. Mater. Chem.* **2002**, *12*, 20.
(87) Besson S.; Gacoin, T.; Ricolleau, C.; Jacquiod, C.; Boilot, J.-P. *Nano Lett.* **2002**, *2*, 409.
(88) Ryoo, R.; Ko, C. H.; Kruk, M.; Antochshuk, V.; Jaroniec, M. *J. Phys. Chem. B* **2000**, *104*, 11465.

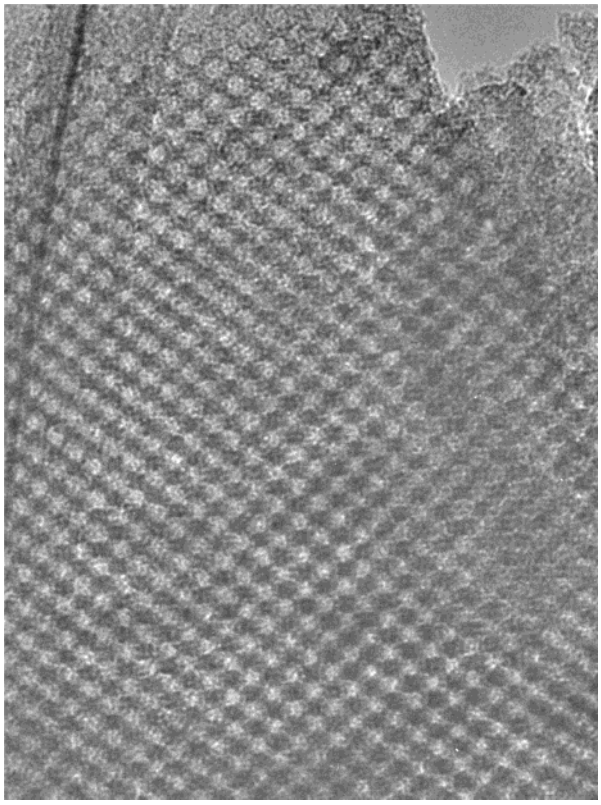

Figure 1. TEM image of FDU-1 structure ([100] incidence of the cubic phase). The image area is ca. 400 nm by 300 nm.

filtered and dried in an oven at 353 K. The resulting samples are denoted X-Bt, where X stands for the symbol of the sample used for the boiling and t denotes the boiling time in hours (h) and days (d). For instance, IId-TMS-C-B4d denotes the sample IId (calcined at 813 K), which was modified with TMS, calcined at 813 K, and finally heated in water for 4 days at 373 K.

Measurements. Nitrogen and argon adsorption measurements were carried out at 77 K using a Micromeritics ASAP 2010 volumetric adsorption analyzer. Before the measurements, the samples were outgassed for at least 2 h at 473 K. In the case of argon adsorption measurements, the saturation vapor pressure corresponding to gas−solid equilibrium (measured during the adsorption run) was used to evaluate the relative pressure.[89]

Calculations. Structural information about the samples under study was determined from nitrogen adsorption data. The BET specific surface area[90] was evaluated from the adsorption data in the relative pressure range from 0.04 to 0.2. The total pore volume[90] was estimated from the amount adsorbed at the relative pressure of 0.99. The micropore volume (V_{mi}), primary mesopore volume (V_p), primary mesopore surface area, and external surface area were evaluated using the α_s plot method, as described in detail elsewhere.[91] The primary mesopores of FDU-1 are defined herein as the ordered, cage-like mesopores. The pore size distributions (PSDs) were evaluated using a method developed for cylindrical pores.[92] Because FDU-1 silicas exhibit spherical rather than cylindrical pores, the pore diameters reported herein are likely to be underestimated by about 2 nm, as can be inferred from our earlier study.[84] The pore diameter (w_d) for one of the FDU-1 silica samples synthesized using the standard procedure (sample IIb) was also calculated using a geometrical equation recently proposed by Ravikovitch and Neimark[93] for materials with face-centered cubic (fcc) structure:

$$w_d = a\left(\frac{6}{\pi}\frac{\epsilon_{me}}{\nu}\right)^{1/3} \quad (1)$$

where a is the unit-cell parameter (taken as 21.6 nm on the basis of our small-angle X-ray scattering study[84] of FDU-1 sample prepared under the same conditions as the sample IIb), ν is the number of spherical pores per unit cell ($\nu = 4$ for the fcc structure) and ϵ_{me} is the volume fraction of ordered mesopores in the structure:

$$\epsilon_{me} = \frac{\rho V_p}{1 + \rho(V_p + V_{mi})} \quad (2)$$

where ρ is the pore wall density (assumed to be 2.2 g cm^{-3}, which is typical for silicas with amorphous frameworks; values of 2.2 and 2.0 g cm^{-3} were reported in the literature for OMSs with cage-like pores[80]). The average pore wall thickness (b) in the fcc structure is determined using the following equation:[93]

$$b = \frac{w_d}{3}\frac{(1 - \epsilon_{me})}{\epsilon_{me}} \quad (3)$$

The minimal wall thickness (b_{min}) is estimated as[93]

$$b_{min} = \frac{a}{\sqrt{2}} - w_d \quad (4)$$

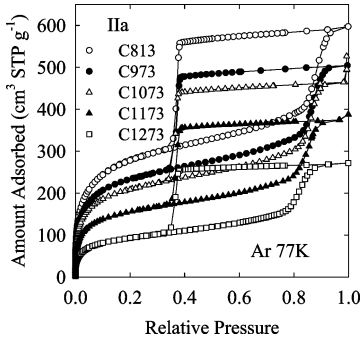

Figure 2. Argon adsorption isotherms for FDU-1 sample IIa calcined at temperatures 813−1273 K.

Results and Discussion

Thermal Stability. Figure 2 shows argon adsorption isotherms for samples of an FDU-1 silica that was synthesized in a two-step procedure involving heating for 6 h at 373 K and which were calcined at different temperatures from 813 to 1273 K. The capillary condensation (which is reflected by the step on the adsorption branch of the isotherm) took place at a quite high relative pressure (above 0.8). Because of the fact that the capillary condensation pressure is an increasing function of the pore diameter, it is clear that the mesopore diameters for these FDU-1 samples were relatively large (on the order of 10 nm). The steepness of the capillary condensation step is indicative of the narrow size distribution of the ordered mesopores. All of the isotherms featured broad adsorption−desorption hysteresis loops that are characteristic of materials with cage-like mesopores. The hysteresis loops closed at a lower pressure limit of adsorption−desorption hyster-

(89) Kruk, M.; Jaroniec, M. *J. Phys. Chem. B* **2002**, *106*, 4732.
(90) Sing, K. S. W.; Everett, D. H.; Haul, R. A. W.; Moscou, L.; Pierotti, R. A.; Rouquerol, J.; Siemieniewska, T. *Pure Appl. Chem.* **1985**, *57*, 603.
(91) Matos, J. R.; Mercuri, L. P.; Kruk, M.; Jaroniec, M. *Langmuir* **2002**, *18*, 884.
(92) Kruk, M.; Jaroniec, M.; Sayari, A. *Langmuir* **1997**, *13*, 6267.
(93) Ravikovitch, P. I.; Neimark, A. V. *Langmuir* **2002**, *18*, 1550.

esis, which is a pressure limit below which the adsorption−desorption process is reversible (in most cases; there are some exceptions, but they are not relevant for the present study), that is, the desorption branch follows the adsorption branch of the isotherm.[90,93−95] The lower limit of hysteresis is characteristic of a given adsorbate and temperature.[90,94,95] In particular, it is located at pressures 0.26−0.38 and 0.40−0.50 for argon and nitrogen, respectively, at 77 K.[94,95] It is known that above the lower pressure limit of adsorption−desorption hysteresis, the capillary evaporation in large cage-like mesopores is delayed (often significantly) with respect to capillary condensation.[90] This is because the capillary condensation from a given pore takes place at a pressure governed by the diameter of the pore interiors, whereas the capillary evaporation (which is reflected by the step on the desorption branch of the isotherm) takes place at a pressure that reflects the diameter of the entrances to the pore.[94,95] More specifically, the capillary evaporation from a given pore connected to the surrounding through narrower connecting pores is delayed to either the relative pressure at which the capillary evaporation occurs in at least one of the connecting pores, or the lower pressure limit of hysteresis, whichever of these two pressures is higher.[95] Because the connecting pores may in some cases be much narrower than the pore interiors, the capillary evaporation from the connecting pores may take place at much lower pressures than that for the capillary condensation in the pore interiors. If the latter capillary condensation takes place significantly above the lower limit of hysteresis, wide hysteresis loops are observed, as in the case of the samples considered herein. The occurrence of desorption at the lower limit of adsorption−desorption hysteresis for argon at 77 K indicates that the size of entrances to the mesopores is below ∼4 nm. This limit was assessed in our experimental study of desorption from model ordered mesoporous silicas[95] and in the computational/experimental studies of Ravikovitch and Neimark.[94]

As can be seen in Figure 2, the increase in the calcination temperature from 813 to 1273 K resulted in lowering of the adsorption capacity and in the shift of the capillary condensation pressure toward smaller relative pressures, which is indicative of lowering of the mesopore diameter. This is a typical behavior of OMSs.[88] The pore size changes can be seen more clearly on the pore size distributions (PSDs) shown in Figure 3. The pore diameter was reduced from 11.3 to 9.5 nm with a concomitant slight reduction of the height of the PSD peak, but there was no broadening of the PSD peak. After the calcination at 1273 K, the specific surface area was reduced to one-third, the total pore volume dropped to less than half, and the micropore volume decreased to one-fifth of their respective values after the calcination at 813 K (see Supporting Table 1S in the Supporting Information). On the other hand, about 60% of the primary mesopore volume and primary mesopore surface area was retained, showing that the ordered mesopores of FDU-1 were preserved after heating at very high temperatures (1173−1273 K). These results on the thermal stability of FDU-1 are similar to the best results for OMSs reported in the literature.[66,70−72] The

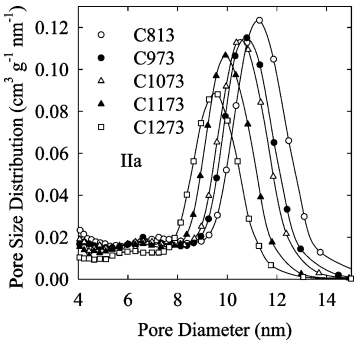

Figure 3. Pore size distributions calculated from nitrogen adsorption isotherms for FDU-1 sample IIa calcined at temperatures 813−1273 K.

thermal stability of two other FDU-1 samples synthesized under the same conditions was tested and similar results were obtained for temperatures up to 1173−1223 K, although a partial or even essentially complete collapse of these samples was observed at 1273 K. It can be concluded that the standard synthesis of FDU-1 (first step at room temperature, and the second-step heating at 373 K for 6 h) affords materials that are stable to 5-hour calcination at 1173−1223 K or even at 1273 K. It was found that the heating step at 373 K during the synthesis was important in obtaining more thermally stable FDU-1 samples. The elimination of this step resulted in lower stability, which manifested itself in a partial collapse at 1173 K and the loss of accessible porosity at 1273 K (see Supporting Figures 1S and 2S in the Supporting Information). It is anticipated that longer heating times or higher temperatures in the second step of the synthesis may further enhance the thermal stability of FDU-1. From the results presented above, it is clear that FDU-1 silicas prepared under appropriate conditions exhibit high thermal stability.

We are aware of only one prior contribution that cast some light on the thermal stability of ordered silicas with large cage-like pores. Namely, it was reported that it was possible to prepare SBA-16 and SBA-11 silica films that were thermally stable up to 1123 K, as inferred from XRD and TEM.[76] However, this study provided little structural information, and, moreover, XRD is not a preferred method to study the stability of OMSs,[42,56,69] as already noted above. So our study provides the first clear experimental evidence that OMSs with large cage-like pores exhibit a facile thermal stability. In general, little work has been reported on the thermal stability of any OMSs with cage-like pores. The only additional report known to us provided information that the structure of SBA-1 silica with *Pm*3*n* symmetry, which was synthesized through an organic-modified ordered silica intermediate, was stable up to 1073 K.[75] So, our results provide new, important insight into the largely unexplored, but potentially practically and theoretically important issues of the thermal stability of the OMSs with cage-like pores.

Hydrothermal Stability. Study of the structural changes caused by boiling in water for different periods of time was carried out on an FDU-1 sample synthesized in a standard procedure and calcined under typical conditions (813 K). Argon adsorption isotherms for the calcined FDU-1 silica before and after boiling for different periods of time ranging from 3 hours to 32 days

(94) Ravikovitch, P. I.; Neimark, A. V. *Langmuir* **2002**, *18*, 9830.
(95) Kruk, M.; Jaroniec, M. *Chem. Mater.* **2003**, *15*, 2942.

Table 1. Structural Properties Determined from Nitrogen Adsorption Data for FDU-1 Sample IIb Before and After Heating in Water at 373 K for Different Periods of Time[a]

sample	S_{BET} ($m^2\ g^{-1}$)	V_t ($cm^3\ g^{-1}$)	w (δ) (nm)	V_{mi} ($cm^3\ g^{-1}$)	S_p ($m^2\ g^{-1}$)	V_p ($cm^3\ g^{-1}$)	S_{ex} ($cm^3\ g^{-1}$)
IIb	920	0.77	10.7 (2.3)	0.29	270	0.44	30
IIb-B3h	720	0.66	10.7 (2.3)	0.20	250	0.42	20
IIb-B6h	680	0.69	10.8 (2.2)	0.16	300	0.48	30
IIb-B12h	660	0.68	11.0 (2.2)	0.15	290	0.48	20
IIb-B1d	630	0.71	11.2 (2.2)	0.13	320	0.54	20
IIb-B2d	610	0.78	11.8 (2.2)	0.09	390	0.64	30
IIb-B4d	570	0.81	12.0 (2.4)	0.06	400	0.70	30
IIb-B8d	450	0.77	12.4 (3.2)	0.04	330	0.67	40
IIb-B16d	400	0.77	12.7 (3.8)	0.03	280	0.66	50
IIb-B32d	300	0.72	13.0 (5.2)	0.00	*b*	*b*	*b*

[a] Notation: S_{BET}, BET specific surface area; V_t, total pore volume; w, primary mesopore diameter (calculated using a method developed for cylindrical rather than spherical pores; the actual pore diameters are likely to be larger by about 2 nm); δ, the width (nm) of the pore size distribution at the half of its height is given in brackets; V_{mi}, micropore volume (including the volume of the connecting pores, if the latter are of diameter below about 4 nm); S_p, primary mesopore surface area; V_p, primary mesopore volume; S_{ex}, external surface area. [b] These parameters could not be determined with a reasonable accuracy using the α_s plot method because of the large pore size and some tailing of the pore size distribution toward larger pore sizes for this sample.

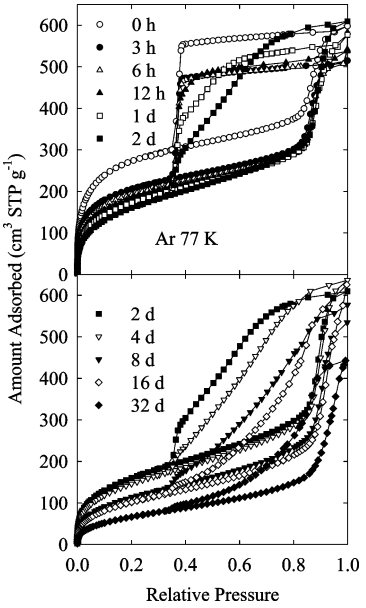

Figure 4. Argon adsorption isotherms for FDU-1 sample IIb before and after boiling for periods of time from 3 hours to 32 days.

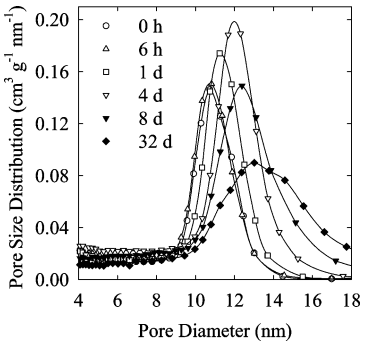

Figure 5. Pore size distributions calculated from nitrogen adsorption isotherms for FDU-1 sample IIb before and after boiling for periods of time from 3 hours to 32 days.

are shown in Figure 4. Structural parameters, such as the specific surface area, pore volume, and pore size for these samples are provided in Table 1. First, several hours of boiling brought about a decrease in the total pore volume and specific surface area, but the pore diameter and the shape of the hysteresis loop remained essentially unchanged (see Figures 4 and 5). However, after 12 or more hours of boiling, a steep decline on the desorption branches of the isotherms started to take place above the lower limit of adsorption−desorption hysteresis (that is, above the relative pressure 0.27−0.38). As mentioned above, this behavior is indicative of the development of pore entrances of size above about 4.0 nm. The proportion of the amounts desorbed above and at the lower limit of hysteresis gradually increased as the boiling was prolonged, which can be interpreted as an evidence that a higher percentage of the ordered mesopores developed an access to the particle's surrounding through continuous pathways of pore entrances wider than ∼4 nm.[95] For longer boiling times, the desorption at the lower limit of hysteresis became less pronounced, and the position of the decline on the desorption branch gradually shifted to higher relative pressures, which is indicative of the gradual enlargement of the pore entrances. Under the assumption that the pore entrances are cylindrical in shape, one can attempt the estimation of their diameter by comparing the position of the decline on the desorption branch of the isotherm with the adsorption−desorption data for ordered mesoporous materials with cylindrical pores. This comparison suggests that the pore entrances, which were below 4 nm before the boiling (as well as after boiling for 6 h or shorter), were enlarged to average diameters of ∼6 and ∼8 nm after 4 and 16 days of boiling, respectively. This crude assessment was made by comparing the position of the midpoint of the capillary evaporation step for FDU-1 samples with the positions of desorption branches of isotherms for MCM-41 and SBA-15 silicas with approximately cylindrical pores (data reported in refs 88 and 89). In the case of these FDU-1 samples, the capillary evaporation extended over broad relative pressure intervals (except for the steep decline at the lower limit of hysteresis), which can be regarded as evidence of the broad size distribution of the pore entrances. A similar observation can be made on the basis of nitrogen adsorption data (see Supporting Figure 3S), but in this case, no information about the pore entrance size enlargement during the boiling for 12 h could be obtained. This is consistent with an earlier conclusion that the analysis of hysteresis loops for argon adsorption at 77 K allows one to obtain information about pore entrances of diameters smaller than those that can be elucidated from the hysteresis

Table 2. Structural Properties Determined from Nitrogen Adsorption Data for FDU-1 Sample IIc Before and After Stabilization and/or Heating in Water at 373 K for 4 Days[a]

sample	S_{BET} ($m^2\ g^{-1}$)	V_t ($cm^3\ g^{-1}$)	w (δ) (nm)	V_{mi} ($cm^3\ g^{-1}$)	S_p ($m^2\ g^{-1}$)	V_p ($cm^3\ g^{-1}$)	S_{ex} ($cm^3\ g^{-1}$)
IIc(-C813)	860	0.74	10.7 (2.3)	0.25	280	0.46	20
IIc-B4	510	0.84	12.3 (2.7)	0.02	410	0.74	50
IIc-TMS-C	660	0.59	10.3 (2.2)	0.18	240	0.37	20
IIc-TMS-C-B4d	410	0.65	11.6 (2.4)	0.02	310	0.56	40
IIc-C1073	600	0.58	9.9 (2.2)	0.12	300	0.51	30
IIc-C1073-B4d	470	0.70	11.3 (2.5)	0.02	380	0.62	40
IIc-C1173	440	0.47	9.6 (2.2)	0.08	250	0.35	20
IIc-C1173-B4d	400	0.56	10.0 (2.5)	0.04	280	0.47	30

[a] Notation: same as Table 1.

loops on nitrogen isotherms measured at 77 K (the limit is ~4 nm for argon and ~5 nm for nitrogen).[94,95] The use of argon adsorption at 77 K to elucidate the pore entrance size has also its drawbacks related to the fact that argon at 77 K does not exhibit capillary condensation in pores of diameter above ~15 nm.[89] Because the occurrence of complete pore filling (for instance through the capillary condensation) is the basis for the calculation of pore size and volume from adsorption data and the prerequisite for the pore connectivity assessment from desorption data, argon adsorption at 77 K is not suitable to probe structures with very large mesopores. On the other hand, nitrogen adsorption at 77 K is free from these limitations.[89] Therefore, it is used herein to investigate whether any very large mesopores were developed during the boiling, for instance as a result of the fusion of adjacent mesopores with the original separating walls removed in the hot aqueous environment. As can be seen in Supporting Figure 3S, the capillary condensation step leveled off quite abruptly in all cases except for the sample boiled for 32 days. This result indicates that the fusion of adjacent pores did not take place to any major extent even after 16 days of boiling, and only after 32 days does this process appear to be pronounced.

Concomitantly with the enlargement of the pore entrances, the mesopore diameter increased to some extent (see Figure 5). Interestingly enough, the height of the peak on PSD increased and there was no appreciable broadening of the peak during the first 4 days of boiling (see values of the peak width in Table 2). The height of the PSD peak started to decline after 8 days of boiling, which was accompanied by a gradual broadening of the peak. However, the monodispersity of the mesopore size was largely retained even after 32 days of boiling.

For the FDU-1 samples subjected to the heating in water at 373 K, the magnitude of the shift in the position of the desorption branch of the isotherm suggests that the pore entrance enlargement took place much faster than the pore diameter increase. A similar phenomenon has already been reported for silica mesocellular foams, and explained as an effect of the preferential removal of silica from the areas adjacent to the pore windows, where the walls are relatively thin.[68] To this end, the average pore wall thickness of the FDU-1 sample IIb is ~6.8 nm, as calculated using eq 3, whereas the minimal wall thickness in the region of the entrances to the ordered mesopores is somewhat higher than ~3.1 nm (the latter being the distance between two adjacent cage-like pores, calculated using eq 4). On the basis of our adsorption results, it is

Scheme 1. Schematic Illustration of Structural Changes in the FDU-1 Silica Structure Caused by Boiling and High-Temperature Calcination

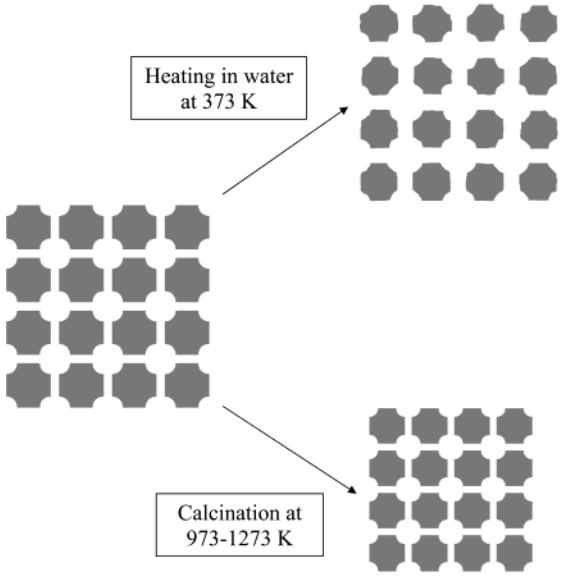

suggested that the boiling in water gradually peels off the silica from the FDU-1 surface (see Scheme 1) and this removal of the outer silica layer progresses much faster in the pore entrance region than in the interior of the mesopore. The exceptional stability of FDU-1 in boiling water is likely to arise from its extremely large wall thickness, especially in the parts of the framework that are crucial for maintaining the integrity of the 3-D wall structure. Similar thick-walled structures were reported for other polymer-templated OMSs with cage-like pores, in particular for SBA-16 with cubic *Im*3*m* structure (body-centered cubic).[57,93] Therefore, one can expect that such OMSs should be inherently highly hydrothermally stable. In the case of these OMSs, the thinner parts of the wall are located at the entrance to the uniform mesopores and its removal does not compromise the integrity of the framework and does not lead to the merging of adjacent pores (as discussed above, there was no evidence of any appreciable merging of FDU-1 mesopores even after 16 days of boiling). On the other hand, typical OMSs with honeycomb (2-D hexagonal) structures (MCM-41,[21,22] FSM-16,[24] and SBA-15)[34] have the thinnest parts of their framework between the adjacent pore channels. The degradation of these thinnest parts not only leads to the merging of adjacent mesopores (which is observed experimentally during boiling),[69] but also to the local loss of connection between the parts of the framework, which may finally lead to the loss of integrity of such 3-D framework

structure. It is suggested that the thickness of the framework in its parts that are necessary for maintaining its integrity is an important factor that determines the stability of OMSs in boiling water.

As far as other structural changes caused by the boiling of FDU-1 are concerned, the specific surface area significantly decreased and the microporosity appeared to be eliminated. On the other hand, the primary mesopore volume and surface area increased during the first 4 days, and subsequently decreased for longer boiling times. The increase in these quantities is consistent with the idea that water washes out a surface layer of silica, which, in the case of the lack of the redeposition of silica and the collapse of the FDU-1 framework, would lead to the increased volume and specific surface area of the ordered mesopores. The total pore volume was relatively constant, although it assumed its peak value after 4 days of boiling and subsequently started decreasing.

It is interesting to note here that the boiling, which enlarges the mesopores and the entrances to them, appears to have a quite opposite effect on the pore size than the high-temperature calcination. The latter decreases the mesopore diameter, as shown above. Moreover, one should note that in contrast to many of the boiled samples, the desorption from the primary mesopores of the samples calcined at higher temperatures took place primarily on the lower limit of adsorption−desorption hysteresis. This is consistent with the contention that there is no pore entrance size enlargement during the high-temperature calcination. In fact, our data (not shown) indicate that the pore entrance size decreases as the calcination temperature increases. The suggested structural changes during the high-temperature calcination and the boiling in water are compared in Scheme 1.

Further Enhancement of FDU-1 Stability. *Introduction of an Additional Silica Layer.* As shown above, the ordered mesoporosity of FDU-1 is exceptionally stable in water at 373 K. On the other hand, the cage-like character of the mesopores is compromised much more easily. This may be a drawback in applications that require a retention of the cage-like pore shape. Therefore, the improvement of the stability of the cage-like structure was attempted using several strategies. The first known strategy is to increase the pore wall thickness through the introduction of an additional layer of silica on the pore surface.[27,33] This can be achieved through the reaction with organosilanes and the subsequent burning out of their organic components[33] or through the surface reaction with TEOS.[27] The first of these options has already been shown to lead to a major hydrothermal stability enhancement for MCM-48 and MCM-41 silicas.[33] Therefore, the surface of FDU-1 was modified with TMS ligands, which were subsequently converted to silica through the calcination under air. This resulted in the introduction of a monolayer (perhaps somewhat less than an equivalent of a compact monolayer) of silica. As can be seen in Supporting Figure 4S, this treatment resulted in a moderate decrease in the adsorption capacity (see also Table 2). The Supporting Figure 5S and Table 2 show that this treatment actually appeared to result in a minor improvement of the hydrothermal stability, because, in this case, the boiling in water resulted in somewhat smaller changes in the structural parameters (the specific surface area, pore volume, and pore size). Moreover, the fraction of cage-like pores that exhibited the desorption on the lower limit of adsorption−desorption hysteresis increased relative to that for the untreated FDU-1.

High-Temperature Calcination. A stabilization effect similar to that described above could be achieved more easily through increasing the calcinations' temperature from 813 to 1073 K. Moreover, the pores of the sample calcined at 1173 K retained much of their cage-like character after the boiling for 4 days. However, this more effective stabilization procedure results in a somewhat more significant decrease in the adsorption capacity. As can be seen in Supporting Figures 6S and 7S, stabilization through silylation/calcination or calcination at 1073 K resulted in the pore size decrease, and the extent of the pore size enlargement upon boiling was only slightly reduced. On the other hand, the FDU-1 sample stabilized through the calcination at 1173 K, which resulted in somewhat more substantial pore diameter reduction, underwent only a minor pore size enlargement during the boiling in water (see Supporting Figure 8S). It was attempted to further increase the stability through the calcination at above 1173 K, but no additional stabilization was observed, and the resultant materials exhibited much lower adsorption capacity. It appears that 1173 K is optimal for the stabilization of the FDU-1 structure (synthesized in a two-step procedure, as described above) through the high-temperature calcination. It should be noted that high-temperature calcination was proposed earlier as a means of the stabilization of large-pore MCM-41 silica.[96] Interestingly enough, in the case of this MCM-41 silica, the indication of improved performance was the structural retention after 3 h of boiling, which is much shorter than the typical boiling times considered herein. Stabilization through the high-temperature calcination is likely to be related to the increased silica framework consolidation. First, this calcination results in an appreciable decrease in microporosity[88] (see Supporting Table 1S and Table 2), which may reduce the extent of penetration of water within the FDU-1 framework. Second, the high-temperature calcination is likely to significantly increase the degree of framework cross-linking, and consequently, to increase the number of siloxane linkages that would have to be hydrolyzed in order to remove the silica species from the FDU-1 surface.

Surface Modification with Organic Groups. It has been reported that surface modification with organic groups is a facile way for the stabilization of OMSs.[33,54−56] Our study showed that surface modification with organosilyl ligands was the most successful approach (among those studied herein) for improvement of the stability of FDU-1 in water at 373 K. Trimethylchlorosilane was used as a modifier, which allows one to chemically bond a monolayer of trimethylsilyl ligands onto the silica surface. The modification led to an appreciable decrease in the adsorption capacity (see Figure 6, Supporting Figures 9S−11S, and Supporting Table 2S). Both modi-

(96) Huo, Q.; Margolese, D. I.; Stucky, G. D. *Chem. Mater.* **1996**, *8*, 1147.

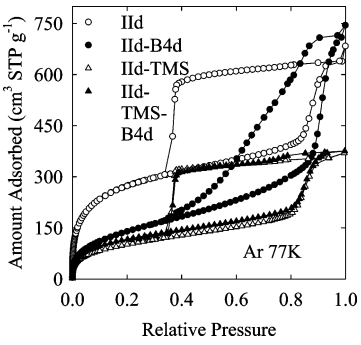

Figure 6. Argon adsorption isotherms for FDU-1 sample IId: (i) calcined at 813 K, and (ii) calcined at 813 K and modified with TMS, before and after boiling for 4 days.

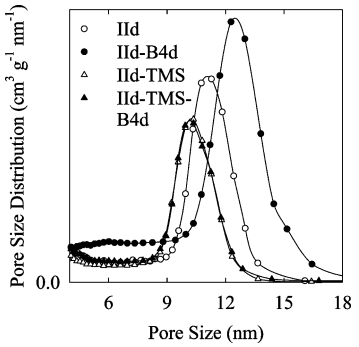

Figure 7. Pore size distributions calculated from nitrogen adsorption isotherms for FDU-1 sample IId: (i) calcined at 813 K, (ii) calcined at 813 K and modified with TMS, before and after boiling for 4 days.

fied and unmodified samples were boiled for 4 days. Boiling of the unmodified FDU-1 sample resulted in a decrease in the specific surface area, enlargement of the pore size, and change of the pore structure from cage-like to much more open. On the other hand, the porous structure of the modified material remained almost unchanged, as can be seen from the PSD data (Figure 7) and from the significant retention of the shape of the hysteresis loop on the argon adsorption isotherm. The structural changes included a small increase in the specific surface area and development of a small fraction of pores with less cage-like character, which can be inferred from the increased steepness of the desorption branch of the isotherm above the lower limit of hysteresis.

The reproducibility of the stabilization effect was verified on two other samples. FDU-1 silica III was synthesized initially at room temperature and then heated for 8 days at 353 K. This sample exhibited pore entrance sizes larger than those for the samples I and IIa−e, because the capillary evaporation (desorption) from its uniform mesopores took place to some extent above the lower limit of hysteresis (see Supporting Figures 9S and 10S). The modification with TMS ligands decreased the adsorption capacity and shifted both the position of the capillary condensation step and the part of the capillary evaporation step above the lower limit of hysteresis to lower pressure values, which revealed the decrease in pore diameter and pore entrance diameter. The unmodified sample III appeared to be less hydrothermally stable than the other FDU-1 samples discussed above. After 4 days of boiling, the pore structure largely lost its original cage-like character, as seen from the narrowness of the hysteresis loop that resembled the adsorption behavior of channel-like rather than cage-like mesopores. Moreover, the primary mesopores were enlarged and their distribution was significantly broadened (see Supporting Figure 12S). On the other hand, the adsorption properties of the TMS-modified sample were changed to a minor extent after the boiling, although the increased steepness of the desorption branch indicates that a fraction of the pore entrances underwent an enlargement. Still, the position of the PSD peak remained essentially unchanged. A similar result was obtained for the FDU-1 sample IIe (see Supporting Figures 11S and 13S). Apparently, the sample was slightly less stable than the sample IId synthesized and modified under the same conditions.

The lack of pore diameter enlargement for the organic-modified FDU-1 after 4 days of boiling indicates that the layer of organosilane groups on the silica surface effectively prevents the erosion of the silica framework. On the other hand, ways of stabilization such as the introduction of an additional layer of silica or high-temperature calcination appear to slow the erosion process to some extent.

Conclusions

FDU-1 exhibits an exceptionally high hydrothermal stability in water at 373 K. The pore size uniformity was retained even after 32 days of boiling, although the pore diameter gradually increased with time of the treatment. Despite the remarkable hydrothermal stability of the uniform mesopores, the entrances to them were noticeably enlarged even after 12 h of boiling, and their size gradually increased as the boiling was prolonged. This resulted in the development of relatively open pore structures after long boiling, which is quite similar to the pore entrance size enlargement observed during the prolonged heating at 373−413 K in a two-step synthesis of FDU-1, which we have reported elsewhere.[84] However, adsorption data suggest that the boiling of calcined FDU-1 results in a broader distribution of pore entrance sizes than that observed after the aforementioned two-step synthesis. The introduction of an additional silica layer on the FDU-1 surface allowed us to further enhance of the hydrothermal stability, but the improvement was small. A similar stabilization effect was also achieved by simply increasing the calcination temperature to 1073 K (from 813 K), whereas the FDU-1 sample calcined at 1173 K was significantly more stable, with its original mesopore structure preserved to an appreciable extent after 4 days of heating in water at 373 K, which would essentially completely destroy structures of the majority of currently known OMSs. This shows that the high-temperature calcination is a facile way to improve the hydrothermal stability of FDU-1. However, it was not beneficial to increase the calcination temperature above 1173 K. The most hydrothermally stable FDU-1 samples were obtained after the surface modification with organosilane ligands. This stabilization method allowed us to obtain an FDU-1 sample with pore structure almost unchanged after 4 days of boiling.

In addition to its remarkable hydrothermal stability, FDU-1 exhibits a facile thermal stability. For samples synthesized with hydrothermal treatment at 373 K, the

uniform mesopore structure was retained to at least 1223 K. In these cases, a significant fraction of the primary mesopore volume was retained up to at least 1173 K, with no appreciable broadening of the pore size distribution. Increase in the calcination temperature led to a gradual reduction of the mesopore size, whereas increase in the boiling time led to a gradual pore size enlargement. These findings demonstrated two new and simple ways to tailor the primary mesopore diameter for FDU-1.

Acknowledgment. M.J. acknowledges support by NSF Grant CHE-0093707. We thank Dr. Rene Geiger from Dow Chemicals for providing the triblock copolymer. Professor Osamu Terasaki (Stockholm University) is gratefully acknowledged for providing TEM images of FDU-1.

Supporting Information Available: Figures (13) with argon adsorption isotherms (5), nitrogen adsorption isotherms (2), and pore size distributions derived from nitrogen adsorption isotherms (6); tables (2) with structural data derived from nitrogen adsorption isotherms (pdf). This material is available free of charge via the Internet at http://pubs.acs.org.

CM034911U